Check for updates

Sulfate-induced large amplitude conformational change in a Solomon link†

Cuong Dat Do, [ID] [a] Dávid Pál, [ID] [a] Andrey Belyaev, [ID] [b] Marion Pupier,[a] Anniina Kiesilä,[b] Elina Kalenius, [ID] [b] Bartomeu Galmés, [ID] [c] Antonio Frontera, [ID] [c] Amalia Poblador-Bahamonde [ID] [a] and Fabien B. L. Cougnon [ID] ‡*[ab]

A doubly-interlocked [2]catenane — or Solomon link — undergoes a complex conformational change upon addition of sulfate in methanol. This transformation generates a single pocket where two SO_4^{2-} anions bind through multiple hydrogen bonds and electrostatic interactions. Despite the close proximity of the two anions, binding is highly cooperative.

Biopolymer conformational changes are essential to many biological processes such as the cooperative binding of four molecules of dioxygen to haemoglobin,[1] and the remote transfer of information mediated by G protein-coupled receptors.[2,3] Taking inspiration from nature, chemists have designed a broad range of synthetic folded molecules, or foldamers,[4–11] able to change conformation.[12–16] However, the propensity of foldamers to unfold in response to external stimuli limits both the diversity and the amplitude of the accessible transformations.[17,18] Non-biomimetic folded molecules such as multiply entangled macrocycles[19–25] may provide a means to solve this issue. Multiply entangled macrocycles can be considered to be folded because the presence of entanglements reduces their conformational freedom and can block them in specific conformational states. Unlike foldamers, these structures cannot unfold unless a covalent bond is broken but can be deformed in the three dimensions of space by moving the individual threads relative to one another. This process, referred to as "Reidemeister moves"[26,27] in mathematics, should in principle allow transitions between multiple conformational states of different shapes and symmetries. Harnessing such complex conformational behaviour would provide unprecedented
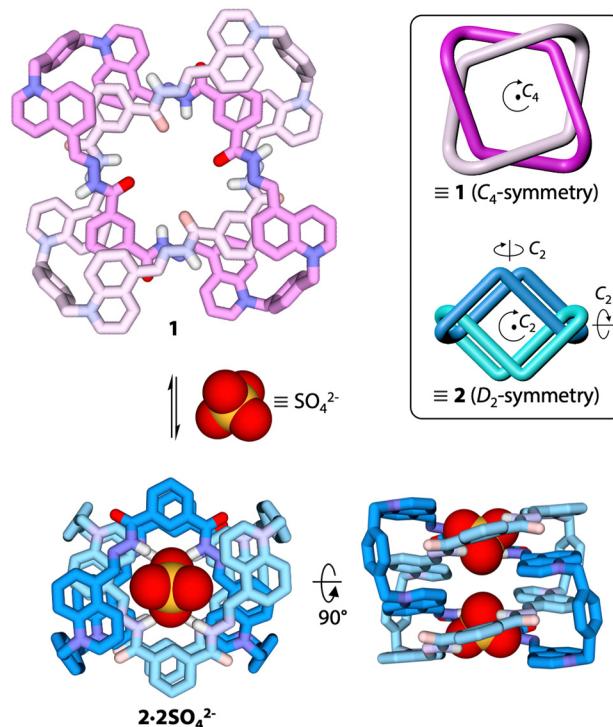
Fig. 1 Sulfate-induced conformational change of a Solomon link in methanol (BP86-D3/def2-TZVP optimized geometries). The insert shows a cartoon representation of conformers **1** and **2**.

opportunities to precisely control the position of functional groups in space and time. Yet, Reidemeister moves have been rarely observed in macromolecules.[28,29]

Our group has recently reported the synthesis of a doubly-interlocked [2]catenane, or Solomon link (**SL**),[30] able to undergo a relatively modest conformational change between two C_4-symmetric states in acetonitrile/water mixtures.[31] We show now that the addition of sulfate to the same Solomon link in methanol triggers a conformational change of greater amplitude (Fig. 1 and Fig. S1, ESI†), which transforms the C_4-symmetric

[a] *Department of Organic Chemistry, University of Geneva, 30 Quai Ernest-Ansermet, 1211 Geneva 4, Switzerland*

[b] *Department of Chemistry, Nanoscience Center, University of Jyväskylä, P.O. Box 35, FI-40014 JYU, Finland. E-mail: fabien.b.l.cougnon@jyu.fi*

[c] *Department de Química, Universitat de les Illes Balears, Carretera de Valldemossa km 7.5, 07122 Palma de Mallorca, Baleares, Spain*

† Electronic supplementary information (ESI) available. See DOI: https://doi.org/10.1039/d3cc04555b

‡ Current address: Department of Chemistry, Nanoscience Center, University of Jyväskylä, P.O. Box 35, FI-40014 JYU, Finland.
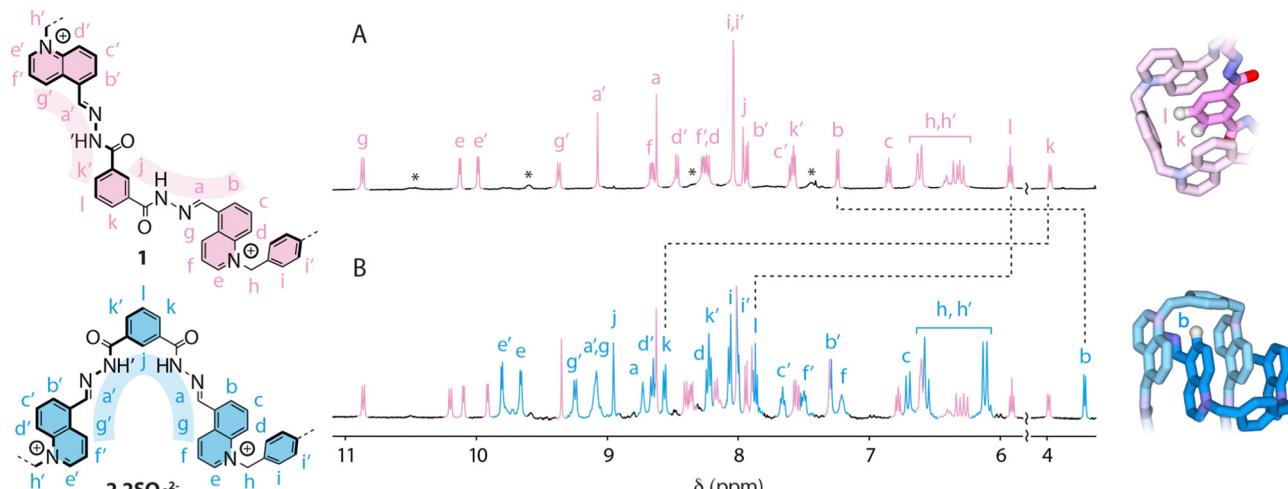
Fig. 2 ^{1}H NMR spectra of the Solomon link (A) before and (B) after addition of 2.6 equiv. of sulfate (CD$_3$OD, 500 MHz, 298 K). The signals corresponding to conformers **1** and **2** are coloured in pink and blue, respectively. The coloured shades on the ChemDraw structure representations highlight key NOE correlations.

conformer **1** previously observed in pure water[31] into a new D_2-symmetric conformer (**2**) different from any of the conformers previously reported. This discovery demonstrates the rich conformational behaviour of multiply entangled macrocycles and establishes their potential as a platform for developing sophisticated multi-responsive systems.

The ^{1}H NMR spectrum of Solomon link **SL^{8+}·8CF$_3$CO$_2^-$** in CD$_3$OD (Fig. 2A) is consistent with conformer **1**. The full NMR characterization is presented in the ESI† (Fig. S2–S5). An optimum packing of the aromatic units results in well-dispersed resonances spreading over *ca.* 7 ppm, from 3.97 ppm to 10.87 ppm. The isophthalic units, each surrounded by two quinoliniums and a xylyl unit, experience a substantial upfield shift. Isophthalic protons **k** (3.97 ppm) and **l** (5.91 ppm) are particularly shielded because they are directly oriented towards the xylyl units in a T-shaped relationship. NOE correlations **j** ↔ **NH** ↔ **a** ↔ **b** and **k′** ↔ **NH′** ↔ **a′** ↔ **g′** recorded in partially non-deuterated CD$_3$OH (Fig. S3, ESI†) show that acylhydrazone protons **NH** and **NH′** point in divergent directions.

The presence of lower intensity, broad signals (labelled with a star in Fig. 2A) indicates the existence of other minor conformers that may be amplified in response to an external stimulus. We reasoned that the addition of an appropriate anion could trigger the amplification of a conformer with a suitable pocket for anion binding, *i.e.*, with all the **NH** and **NH′** hydrogen-bond donors converging towards the centre of the cavity. This hypothesis was tested by carrying out ^{1}H NMR titrations with a range of common anions (Cl$^-$, Br$^-$, I$^-$, CF$_3$SO$_3^-$, PF$_6^-$, SCN$^-$, NO$_3^-$, ReO$_4^-$, ClO$_4^-$, and SO$_4^{2-}$ as tetra-*n*-butylammonium salts, Fig. S6, ESI†).

None of the anions tested induced any response with the notable exception of SO$_4^{2-}$. The addition of sulfate led to the appearance of a new set of signals corresponding to D_2-symmetric conformer **2** (Fig. 2B), which was fully characterized in solution by NMR (Fig. S9–S12, ESI†) and modeled using dispersion-corrected

DFT (BP86-D3/def2-TZVP) methodology.[32,33] Upon binding to sulfate, the Solomon link undergoes a large amplitude conformational change that carries atoms across up to 1.6 nm (Fig. S1, ESI†). In conformation **2**, the quinolinium units stack on each side of the Solomon link. The protons of the quinoliniums buried in the stack (**b–g**) are significantly shielded compared to those of the quinoliniums located on the outer surface (**b′–g′**). Quinolinium proton **b** is the most upfield shifted signal (δ = 3.74 ppm) because it is facing the xylyl unit in a T-shape relationship. The isophthalic units are entirely exposed to the solvent and no longer experience the characteristic shielding observed in conformation **1**. Finally, NOE correlations **g** ↔ **a** ↔ **NH** ↔ **j** ↔ **NH′** ↔ **a′** ↔ **g′** (Fig. S10, ESI†) confirm that both acylhydrazone **NH** and **NH′** hydrogen bond donors are oriented towards the centre of the cavity of **2**, providing an ideal binding site where sulfate can nest.

Electrospray ionization mass spectrometry (ESI-HRMS) corroborates that the Solomon link preferentially binds SO$_4^{2-}$ over the other anions tested (Fig. S13–S15, ESI†), as observed by NMR. More importantly, peaks at m/z 624.2026 and m/z 831.9337, corresponding to [**SL** + 2SO$_4$]$^{4+}$ and [**SL**-H + 2SO$_4$]$^{3+}$, respectively, disclose that the Solomon link binds two equivalents of sulfate (Fig. 3). The central cavity of conformer **2** displays two identical sites where SO$_4^{2-}$ can bind *via* the formation of four N–H⋯O–S and ten C–H⋯O–S hydrogen bonds (Fig. S1, ESI†). The tetrahedral disposition of the four acylhydrazone NH hydrogen bond donors of each binding site nicely matches the tetrahedral geometry of the dianion. The preferential binding of SO$_4^{2-}$ may thus be explained, at least partially, by the high complementarity between the dianion and the binding sites, in terms of size and geometry. The absence of response with the tetrahedral monoanions ReO$_4^-$ and ClO$_4^-$ is likely explained by a weaker electrostatic interaction.

Conformers **1** and **2** slowly exchange on the NMR timescale. The fraction θ of sulfate-bound conformer **2** can therefore be easily measured from the relative integration of the NMR
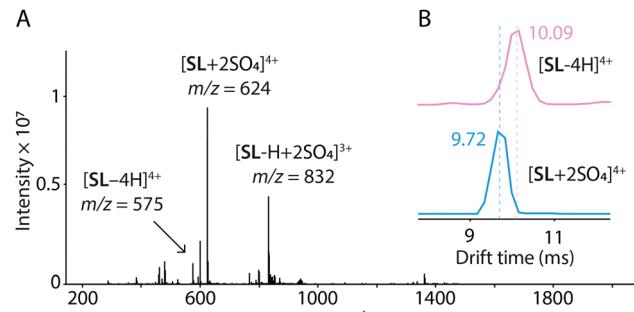
Fig. 3 (A) (+)ESI-MS spectrum of the Solomon link after addition of sulfate (1 : 1 molar ratio, 1 μM each) in CH$_3$OH. (B) Representation of the ion-mobility mass spectrometry drift times and arrival time distributions at m/z 575 and 624, corresponding to ions [**SL**-4H]$^{4+}$ (in pink) and [**SL** + 2SO$_4$]$^{4+}$ (in blue), respectively.

signals as a function of the total concentration of sulfate [SO$_4^{2-}$]. The Hill coefficient $n_H \approx 2$ obtained from the plot $\log\theta/(1 - \theta) = f(\log[\text{SO}_4^{2-}])$ indicates strong positive cooperativity[34] (Fig. 4A). The narrow concentration window in which the transition occurs (Fig. 4A, insert) supports this conclusion. This result is unexpected as the second binding event creates unfavourable electrostatic interactions between the two anions, constrained in close proximity within a single pocket.[35,36] The occurrence of positive cooperativity may be rationalised by considering that the conformational change triggered by the first molecule of sulfate brings all the hydrogen bond donor components of the second binding site (CHs and NHs) in the correct position to bind the second molecule of sulfate, considerably enhancing affinity for the subsequent binding event ($K_1 \ll K_2$). The electrostatic repulsion between the two anions is presumably offset by both the formation of multiple hydrogen bonds and attractive electrostatic interactions between the anions and the polycationic Solomon link.

The affinity of the Solomon link for sulfate, extrapolated from the Hill plot, is highly dependent on temperature. The overall association constant $\beta = K_1 \cdot K_2$ is weak at 263 K ($\beta = 13$ M^{-2}) and increases with temperature ($\beta = 6.8 \times 10^3$ M^{-2} at 313 K). Van't Hoff analysis (Fig. 4B) shows that binding is entropically driven ($\Delta S^\circ = +348 \pm 10$ J mol^{-1} K^{-1}, $\Delta H^\circ = +86 \pm 4$ kJ mol^{-1}). The switch can thus be efficiently operated by changing temperature between 263 K and 313 K in the presence of a small excess of SO$_4^{2-}$ (2.6 equiv., Fig. 4C). Sulfate-bound conformer **2** is favoured at high temperature. The host–guest complex dissociates when the temperature decreases, and the Solomon link switches back to conformer **1**.

Sulfate-bound conformer **2** was only observed in methanol and not in other solvents such as acetonitrile and water (Fig. S21–S22, ESI†), which stabilise better the other conformers.[31] Even the presence of small amounts of water in methanol interferes with the formation of the host–guest complex (Fig. S23, ESI†). It is also interesting to note that the transformation **1** → **2** results in a contraction of the Solomon link detectable by both diffusion spectroscopy (DOSY) and ion-mobility mass spectrometry (IM-MS). During the conformational change, an increase in
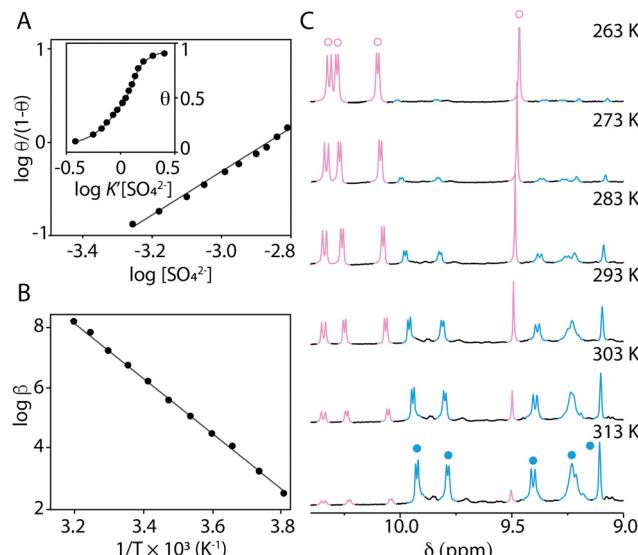

Fig. 4 (A) Hill plot obtained from a titration of SO$_4^{2-}$ into a CD$_3$OD solution of the Solomon link at 313 K. The insert shows the corresponding speciation curve.[34] In this plot, [SO$_4^{2-}$] is normalized by the apparent equilibrium constant K' corresponding to the concentration of SO$_4^{2-}$ producing half-occupation. (B) Van't Hoff plot. (C) Variable temperature ^{1}H NMR spectra of the Solomon link after addition of 2.6 equiv. of sulfate (CD$_3$OD, 500 MHz). The signals corresponding to conformers **1** and **2** are coloured in pink (○) and blue (●), respectively.

diffusion coefficient indicates a decrease in *ca.* 30% of the Solomon link bulk volume consistent with the values measured from the molecular models (Fig. S24, ESI†). The contraction is also evidenced by IM-MS. A clear decrease in experimental collision cross-section values measured upon binding of the two equiv. of sulfate confirms that sulfate-bound conformer **2** is more compact ($^{DT}CCS_{He} = 395.4$ Å^2 for [**SL**-4H]$^{4+}$ *vs.* 378.8 Å^2 for [**SL** + 2SO$_4$]$^{4+}$, see Table S2 for details, ESI†). Here again, the experimental $^{DT}CCS_{He}$ measured for [**SL** + 2SO$_4$]$^{4+}$ closely corresponds to the theoretical $^{TMLJ}CCS_{He}$ value of 373.5 Å^2 calculated from the optimized DFT structure. The host–guest complexes formed with other anions are observed with lower abundance and display larger $^{DT}CCS_{He}$ values compared to [**SL**-4H]$^{4+}$, indicating exclusion complexation. The conformational change thus appears to be specific to SO$_4^{2-}$ both in solution and in the gas phase.

The Solomon link is a remarkably polymorphic molecule, able to undergo either medium (as previously reported)[31] or large amplitude deformations, depending on the experimental conditions. We have now identified three different conformers, whose NMR features are compared in Fig. S25 (ESI†). The protean behaviour of the Solomon link, reminiscent of that of biomolecules, is considerably more complex than that of topologically simpler macromolecules. Such findings may thus lay the groundwork for the design of increasingly sophisticated entangled macrocycles that can change their three-dimensional shape, and perhaps their function, in response to multiple stimuli.

Conflicts of interest

The authors declare no conflict of interest.

Notes and references

1 M. F. Perutz, *Nature*, 1972, **237**, 495–499.
2 D. M. Rosenbaum, S. G. Rasmussen and B. K. Kobilka, *Nature*, 2009, **459**, 356–363.
3 D. M. Thal, A. Glukhova, P. M. Sexton and A. Christopoulos, *Nature*, 2018, **559**, 45–53.
4 E. A. John, C. J. Massena and O. B. Berryman, *Chem. Rev.*, 2020, **120**, 2759–2782.
5 S. Rinaldi, *Molecules*, 2020, **25**, 3276.
6 E. Yashima, N. Ousaka, D. Taura, K. Shimomura, T. Ikai and K. Maeda, *Chem. Rev.*, 2016, **116**, 13752–13990.
7 C. M. Goodman, S. Choi, S. Shandler and W. F. DeGrado, *Nat. Chem. Biol.*, 2007, **3**, 252–262.
8 Y. Ferrand and I. Huc, *Acc. Chem. Res.*, 2018, **51**, 970–977.
9 D. Mazzier, S. De, B. Wicher, V. Maurizot and I. Huc, *Angew. Chem., Int. Ed.*, 2020, **59**, 1606–1610.
10 C. G. Pappas, P. K. Mandal, B. Liu, B. Kauffmann, X. M. Miao, D. Komaromy, W. Hoffmann, C. Manz, R. Chang, K. Liu, K. Pagel, I. Huc and S. Otto, *Nat. Chem.*, 2020, **12**, 1180–1186.
11 Y. Jin, P. K. Mandal, J. Wu, N. Bocher, I. Huc and S. Otto, *J. Am. Chem. Soc.*, 2023, **145**, 2822–2829.
12 R. Rodriguez, E. Suarez-Picado, E. Quinoa, R. Riguera and F. Freire, *Angew. Chem., Int. Ed.*, 2020, **59**, 8616–8622.
13 J. Atcher, P. Mateus, B. Kauffmann, F. Rosu, V. Maurizot and I. Huc, *Angew. Chem., Int. Ed.*, 2021, **60**, 2574–2577.
14 D. Pijper and B. L. Feringa, *Angew. Chem., Int. Ed.*, 2007, **46**, 3693–3696.
15 T. Miyagawa, A. Furuko, K. Maeda, H. Katagiri, Y. Furusho and E. Yashima, *J. Am. Chem. Soc.*, 2005, **127**, 5018–5019.
16 B. A. Le Bailly and J. Clayden, *Chem. Commun.*, 2016, **52**, 4852–4863.
17 Z. Yu and S. Hecht, *Angew. Chem., Int. Ed.*, 2011, **50**, 1640–1643.
18 F. C. Parks, Y. Liu, S. Debnath, S. R. Stutsman, K. Raghavachari and A. H. Flood, *J. Am. Chem. Soc.*, 2018, **140**, 17711–17723.
19 S. R. Beeren, C. T. McTernan and F. Schaufelberger, *Chem*, 2023, **9**, 1378–1412.
20 W.-X. Gao, H.-J. Feng, B.-B. Guo, Y. Lu and G.-X. Jin, *Chem. Rev.*, 2020, **120**, 6288–6325.
21 S. D. P. Fielden, D. A. Leigh and S. L. Woltering, *Angew. Chem., Int. Ed.*, 2017, **56**, 11166–11194.
22 R. S. Forgan, J. P. Sauvage and J. F. Stoddart, *Chem. Rev.*, 2011, **111**, 5434–5464.
23 Z. Ashbridge, E. Kreidt, L. Pirvu, F. Schaufelberger, J. H. Stenlid, F. Abild-Pedersen and D. A. Leigh, *Science*, 2022, **375**, 1035–1041.
24 Y. Inomata, T. Sawada and M. Fujita, *J. Am. Chem. Soc.*, 2021, **143**, 16734–16739.
25 H.-N. Zhang, H.-J. Feng, Y.-J. Lin and G.-X. Jin, *J. Am. Chem. Soc.*, 2023, **145**, 4746–4756.
26 K. Reidemeister, *Abh. Math. Semin. Univ. Hambg.*, 1927, **5**, 24–32.
27 J. W. Alexander and G. B. Briggs, *Ann. Math.*, 1926, **28**, 562–586.
28 J. P. Carpenter, C. T. McTernan, J. L. Greenfield, R. Lavendomme, T. K. Ronson and J. R. Nitschke, *Chem*, 2021, **7**, 1534–1543.
29 V. Marcos, A. J. Stephens, J. Jaramillo-Garcia, A. L. Nussbaumer, S. L. Woltering, A. Valero, J. F. Lemonnier, I. J. Vitorica-Yrezabal and D. A. Leigh, *Science*, 2016, **352**, 1555–1559.
30 F. B. L. Cougnon, K. Caprice, M. Pupier, A. Bauzá and A. Frontera, *J. Am. Chem. Soc.*, 2018, **140**, 12442–12450.
31 K. Caprice, M. Pupier, A. Bauzá, A. Frontera and F. B. L. Cougnon, *Angew. Chem., Int. Ed.*, 2019, **58**, 8053–8057.
32 A. D. Becke, *Phys. Rev. A: At., Mol., Opt. Phys.*, 1988, **38**, 3098–3100.
33 A. Schäfer, C. Huber and R. Ahlrichs, *J. Chem. Phys.*, 1994, **100**, 5829–5835.
34 C. A. Hunter and H. L. Anderson, *Angew. Chem., Int. Ed.*, 2009, **48**, 7488–7499.
35 W. Zhao, A. H. Flood and N. G. White, *Chem. Soc. Rev.*, 2020, **49**, 7893–7906.
36 Q. He, P. Tu and J. L. Sessler, *Chem*, 2018, **4**, 46–93.